

## LATE PLEISTOCENE-HOLOCENE PLANKTONIC FORAMINIFERA FROM THE EASTERN MEDITERRANEAN SEA: TOWARDS A HIGH-RESOLUTION PLANKTONIC FORAMINIFERAL ASSEMBLAGE ZONATION FOR THE LATE QUATERNARY OF THE MEDITERRANEAN.

MARIA SPERANZA PRINCIPATO

*Received May 18, 2001; accepted October 29, 2002*

**Keywords:** Late Pleistocene-Holocene; eastern Mediterranean; planktonic foraminifera; assemblage zones; S1 sapropel.

**Abstract.** A quantitative study of planktonic foraminiferal assemblages has been performed on 7 box cores from different areas of the eastern Mediterranean. This study allowed to reconstruct a high resolution biostratigraphic scheme of the eastern basin for the late Pleistocene/ Holocene. In particular, 6 planktonic foraminiferal assemblage zones have been recognised during the last 18 kyrs, based on the most significant assemblages changes. The chronological framework is defined by a well dated tephra layer (Z2) and permits to calculate an average sedimentation rate for one of the studied cores (BC19). Similar changes in planktonic foraminiferal assemblages are identifiable in wide areas of the Eastern Mediterranean, although records of individual species may show important regional patterns. The comparison between the assemblage zones here defined for the eastern Mediterranean and the existing biozonation for the central Mediterranean shows that similar changes in planktonic microfauna occurred throughout the Mediterranean area during the investigated time slice.

**Riassunto.** Nel presente lavoro vengono presentati i risultati di uno studio quantitativo sui foraminiferi planctonici di 7 box-cores prelevati in varie aree del Mediterraneo orientale. Da questo studio è stato ricavato uno schema biostratigrafico ad alta risoluzione applicabile a tutto il Bacino orientale nell'intervallo tardo Pleistocene/Olocene. In particolare, sono state definite 6 cenozone a foraminiferi planctonici per gli ultimi 18.000 anni, sulla base dei cambiamenti di associazione più significativi. Lo schema cronologico adottato è stato basato su un tephra di età nota (Z2) ed ha permesso di calcolare una velocità di sedimentazione media per una delle carote studiate (BC19). Alcuni cambiamenti nelle associazioni a foraminiferi planctonici ricorrono in vaste aree del Mediterraneo orientale, anche se la distribuzione di particolari specie può presentare talvolta delle caratteristiche regionali. Il confronto tra le cenozone definite in questo lavoro per il Mediterraneo orientale e la biozonazione già esistente per il Mediterraneo centrale dimostra che in gran parte della regione mediterranea si sono verificati cambiamenti simili nella microfauna planctonica durante tutto il periodo considerato.

### Introduction

The interval from the Last Glacial Maximum (18 kyrs BP) to the Present is characterised by climate fluctua-

tations recorded by planktonic biota. The succession of different climatic regimes has determined variations in the physical and chemical properties of water column that are recorded by changes in abundance of the most sensitive foraminiferal species and by the oxygen and carbon isotopic composition of calcareous tests of foraminifera. Distribution and abundance of planktonic foraminiferal species are related to temperature, salinity, availability of nutrients in the water column, thickness of the mixing layer and other biological and paleoceanographic factors. For this reason quantitative analyses of foraminiferal assemblages in sediments can lead to reliable and detailed palaeoclimatic and palaeoceanographic reconstruction for the last glacial cycle.

At present a high resolution biostratigraphic scheme, based on planktonic foraminiferal studies, is established for western and central Mediterranean late Quaternary (Pujol & Vergnaud-Grazzini 1989; Jorissen et al. 1993; Capotondi et al. 1999). These studies apply the "ecozonal methodology" used in palaeoceanographic research since 1989 (Capotondi et al. 1989; Borsetti et al. 1995; Capotondi 1995; Capotondi & Morigi 1996; Capotondi et al. 1999). Ten ecozones have been identified during the last 23 kyrs in the Tyrrhenian Sea and eight ecozones in the Adriatic Sea during the last 15 kyrs (Capotondi et al. 1999).

Sedimentation rate in the eastern Mediterranean is generally low (3-4 cm/1000 yrs), and as a consequence, only few high-resolution studies exist for the last 15 kyrs BP (Vergnaud-Grazzini et al. 1988; Pujol & Vergnaud-Grazzini 1989; Troelstra et al. 1991 among others).

The primary aim of the present study is to provide a detailed palaeoecological-biostratigraphic scheme for the eastern Mediterranean (Ionian and Levantine Basins), using planktonic foraminiferal distribution.

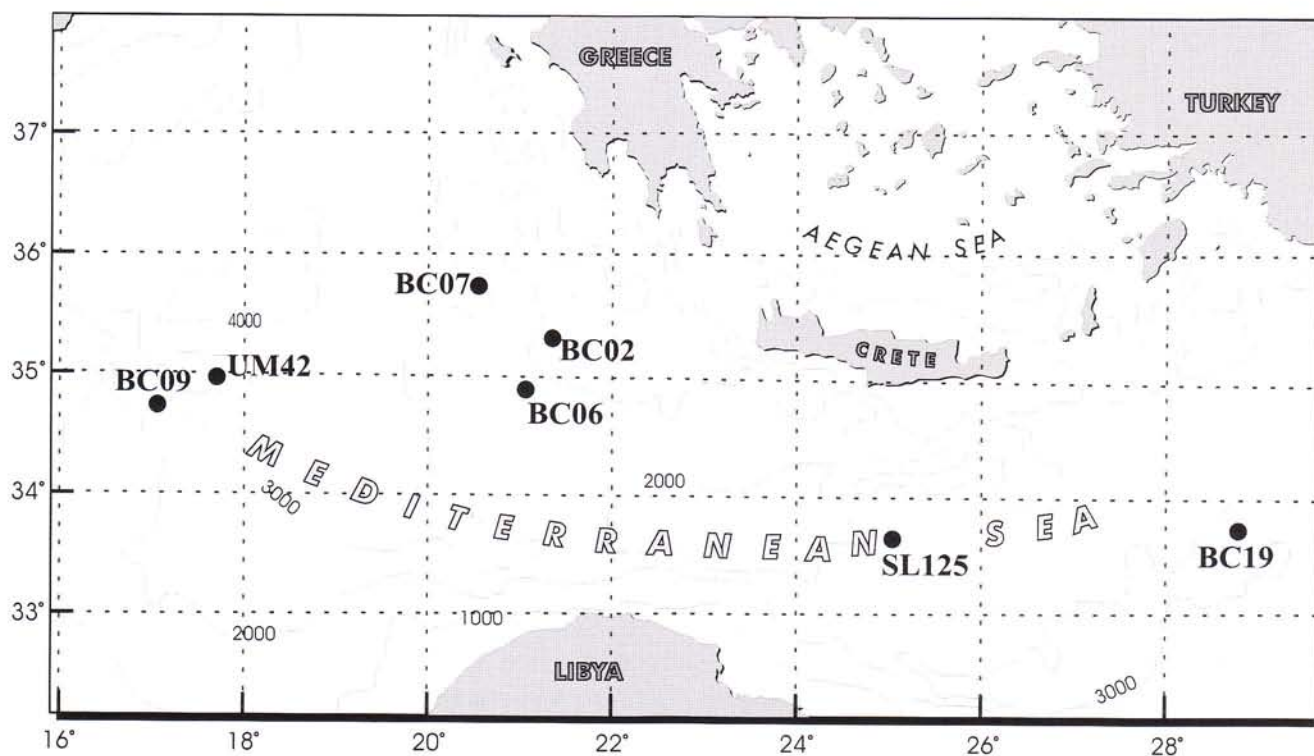


Fig. 1 - Location map of studied cores. Black dots indicate the location of the studied box-cores.

Results obtained for the eastern Mediterranean will be compared with the existing data from the central Mediterranean to attempt a correlation between different sub-basins.

Since the deposition of sapropel S1 is one of the most relevant depositional events in the Mediterranean during the last 10,000 years, some details about sapro-

pels are here reported with a short history of studies related to S1.

Sapropels were defined by Kidd et al. (1978) as sharply-bordered, dark-coloured sedimentary layers with an organic carbon ( $C_{org}$ ) content  $> 2$  wt % and a thickness  $> 1$  cm. Such sediments are also rich in S and abundant redox-sensitive trace metals (Calvert 1983). It

CRUISE	CORE	LOCATION	Latitude N	Longitude E	Water depth (m)	Recovery (cm)
Urania 1997	BC09	Medina Rise	34°55'39"(GPS)	17°04'08"(GPS)	1072	41
Urania 1997	BC07	Mediterranean Ridge	35°45'35"(GPS)	20°32'40"(GPS)	3022	49
Urania 1997	BC06	Mediterranean Ridge	34°52'30"(GPS)	21°07'08"(GPS)	2539	49
Urania 1997	BC02	Plateau between Urania and Atalante	35°17'09"(GPS)	21°24'55"(GPS)	3349	39
Urania 1994	UM42	Medina Rise	34°57'13"(GPS)	17°51'45"(GPS)	1375	35
Marion Dufresne'91	BC19	Tyro Site Abyssal hill	33°47'30"(GPS)	28°36'30"(GPS)	2750	35
Logachev 1999	SL125	Moscow Dome	33°39'24"(GPS)	24°32'58"(GPS)	1946	41

Tab. 1 - Location of studied cores: coordinates, water depth and recovery

is well-known that sapropels are associated with high-amplitude precession minima, characterised by intensified monsoonal circulation (Rossignol-Strick 1985; Hilgen 1991a,b; Hilgen et al. 1993; Vergnaud-Grazzini et al. 1993; Emeis and Shipboard Scientific Party 1996).

The youngest (early Holocene) sapropel is coded as S1 (Cita et al. 1977). Recently, as a result of the work carried out by Hilgen, Lourens and others (Lourens et al. 1996), the ages of individual sapropels were assigned using a lag-time of 3 kyrs between sapropel formation and its correspondent precession minimum (insolation index). According to this new nomenclature (*i*-cycle code) the sapropel S1 becomes Si2 because of its correspondence with the insolation cycle 2. Anyway it is common to use the old nomenclature for the Holocene sapropel S1 (Si2) yet and so the most recent sapropel of the Mediterranean will be called S1 in this study.

The time of S1 formation falls between approximately 9000 and 6000 yrs BP. The deposition of this sapropel started during the Holocene Climatic Optimum, which followed the last major retreat of the Northern Hemisphere continental ice sheets. S1 correlates with an interval of oxygen isotope Stage 1 and it is generally up to 20 cm thick (Stanley & Maldonado 1977). According to Cita et al. (1982), this level has an organic-carbon content of approximately 2%.

It was recently demonstrated (De Lange et al. 1989; Van Santvoort et al. 1996; Van Santvoort & De Lange 1997) that post-depositional oxic diagenesis controls the changes in thickness and consequent deposi-

tion of sapropel S1. On the basis of these data, it was also demonstrated that substantial amounts of the original high  $C_{org}$  content could be removed from the upper level of the S1 unit by post-depositional oxidation (Thomson et al. 1999). Organic carbon removal may, in some extreme cases, leave only a "ghost" of sapropel (Thomson et al. 1995). As a consequence, we can assume that sapropel S1 was originally thicker. This may imply a longer duration of sapropel S1 formation (5-9 kys BP instead of 7-9 kyrs BP). The downward diffusion of bottom water oxygen in an oxidation front leads to the formation of Mn and Fe oxyhydroxide peaks. The most recent Mn peak is normally useful to identify the original top of S1. Diffuse dark brown bands, a few cm thick, are often found immediately above and 6-8 cm above the visual top of sapropel. This brown colour is characteristic of Mn oxyhydroxide enrichments. Thomson et al. (1995) and Van Santvoort et al. (1996) demonstrated that Barium provides a quantitative proxy for the S1 sapropel. High values of the Ba profile are considered to represent the entire period of high productivity during the formation of S1. In fact a correlation exists between the settling fluxes of  $C_{org}$  and Ba intercepted by sediment traps, even if the mechanism producing the association of the two elements in the water column is poorly understood (Dymond & Collier 1996).

#### Material and methods

Seven box cores were studied from different areas of the Eastern Mediterranean Sea (Tab.1, Fig.1). The material was collected dur-

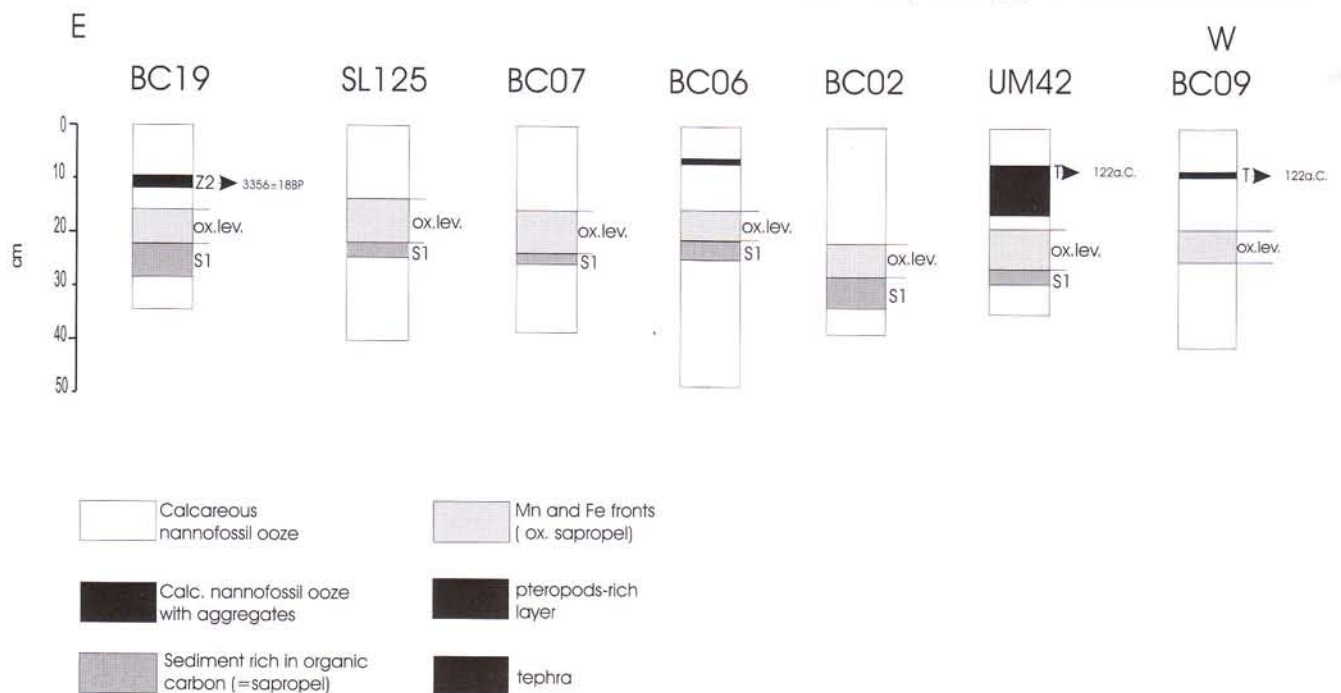


Fig. 2 - Lithological description of studied cores. The age of tephra layers is also indicate.

ing different cruises:

- SL125: Logachev 1999 Smilelabel cruise;
- BC09, BC07, BC06, BC02: Urania 1997 SIN/SAP cruise;
- UM42: Urania 1994 Paleoflux cruise;
- BC19: Marion Dufresne 1991 MD69 Marflux cruise.

Most cores consist mainly of hemipelagic "calcareous ooze".

The Holocene part of most cores (with the exception of the box core BC09 in the Medina Rise) contains a well-developed S1 sapropel.

Two hundred and seventy-two samples were investigated. All samples were taken at intervals of 1 cm, following the most important changes in colour and lithology of sediments.

Each sample was dried at 50 °C and washed with 63 µm, 150 µm and 500 µm mesh sieves. The fraction 150-500 µm was split in an aliquot of about 300 planktonic foraminifera.

The >150 µm fraction used in this study clearly record trends from the most significant planktonic foraminiferal species whereas the same signals can be attenuated considering the total fraction >63 µm that is dominated by juvenile forms and by the species *T. quinqueloba*. Anyway the comparison with >63 µm fraction data (Capotondi et al. 1999) was performed in this study to test if some significant trends of planktonic foraminiferal species are really recognisable in the total foraminiferal assemblage.

Specimens from the selected fraction >150 µm were then identified and counted. Raw data were quantified as a percentage of the total number of planktonic and benthic foraminifera, largely following the taxonomic concept of Hemleben et al. (1989). All morphotypes of *Globigerinoides ruber* are lumped together. Only the *alba* and *rosea* varieties are distinguished. *Globigerinoides sacculifer* group includes also *G. trilobus*, according to the taxonomic concept of Hemleben et al. (1989), and the species *Globoturbotalita rubescens* and *G. tenella* are lumped together because of similar ecological characteristics. Groupings simplify the graphical representations, without altering the proposed ecozonal scheme.

The tephra layers recognised in 3 box cores were identified by glass fragments composition with Energy Dispersion Scansion (EDS) analyses. Two sand fractions (63-150; >150 µm) were separated. Aggregates were separated by ultrasounds (BC09 and UM42). All fractions were cleaned with HCl solution to dissolve carbonates and concentrate volcanic silica. These were then included in epoxy resin ("araldite") and polished. The obtained data were interpreted by Dr. L. Vezzoli (Insubria University).

### Lithostratigraphy and tephrochronology

The seven studied box-cores are located in the Ionian Sea and in the Levantine Basin along a West-East transect (Fig. 1).

Fig. 2 shows the lithology of the studied box-cores as follows (from bottom to top):

"sediments below sapropel S1" are pelagic and hemipelagic sediments. They could be defined calcareous nannofossil oozes, with the exception of BC09 box core where coarse detritic fragments are also present. Pyrite can partially cover shells of foraminifera in sediments just below S1. This colour is usually grey in the interval just below sapropel S1, whereas it changes to brown-olive brown, in the lower part of the core;

"sediments of sapropel S1" are characterised by abundant biogenic sand fraction (up to 50%). This sapropel is also characterised by a few characteristic minerals such as pyrite in aggregates and/or attached to foraminifera and pteropod - shells, phosphate fragments such as fish teeth and gypsum crystals. The presence of

gypsum is usually accompanied by the disappearance of pteropod - shells. The colour of these sediments is usually brownish black, olive black to totally black. The thickness of this layer in the studied cores varies, from 2 cm (BC07) to about 6 cm (BC19); this level is totally absent in the box core BC09;

"oxidised sediments above sapropel S1": this interval is visible in all the studied box cores and its identification was mostly based on the clear change in the colour of sediments. According to Freydier et al. (2001), the thickness of barium profiles was used to define the original extension of sapropel and the exact thickness of the oxidised level in BC19 and UM42 box cores. The sand fraction in these sediments is mostly characterised by foraminiferal shells because of disappearance of pteropods and by the presence of gypsum crystals in most intervals. Foraminiferal shells, sometimes partly pyritized, are often filled with oxides and therefore they can appear orange in colour. The lower part of this lithostratigraphic interval is usually darker, becoming yellowish (and/or olive) brown up to totally brown-upwards;

"pelagic sediments above the oxidised layer" are homogeneous (calcareous nannofossil ooze) and deposited in oxic conditions. The sand fraction can be rich in pteropod shells, increasing the sediment grain-size. Lithic calcareous fragments are present in box-core BC09. The colour of these sediments is normally brown-yellowish brown. In box-core UM42 this latter interval contains lithic aggregates, probably related to reworking processes. According to oxygen isotope variations and <sup>14</sup>C AMS analyses performed on *G. ruber* (De Lange pers. comm.), it is evident that the 10 cm above S1 sapropel are characterised by redepositional processes. The supposed reworked level in UM42 was identified also by the abundance of *G. scitula*. This sub-polar species (Bè & Tolderlund 1971) is usually absent in Holocene sediments from eastern Mediterranean and is abundant in the whole Mediterranean during the Last Glacial Maximum (Capotondi et al. 1999; Saffi et al. 2001);

"cineritic levels (tephra)": the tephra, recovered in UM42 and BC09 box cores and called "T" in this paper, is characterised by mineral aggregates, brown or red in colour, and few glass fragments visible in the sand fraction (>63 µm). This tephra can be related to a basaltic Plinian eruption from Etna, occurred in 122 B.C. (Coltelli et al. 1998). In particular, it contains plagioclases, quartz, pyroxenes and ilmenite, and glass fragments have benmoreite-mugearite composition.

The tephra layer recovered in BC19 box-core is identified as "Z2" (Fig. 2) because of acid composition of glass fragments (riolites) and correlated with the 3356 ± 18 yrs <sup>14</sup>C BP Santorini eruption (De Rijk et al. 1999). This level is mostly composed of glass fragments, foraminifer and pteropod shells appear diluted in sediment.

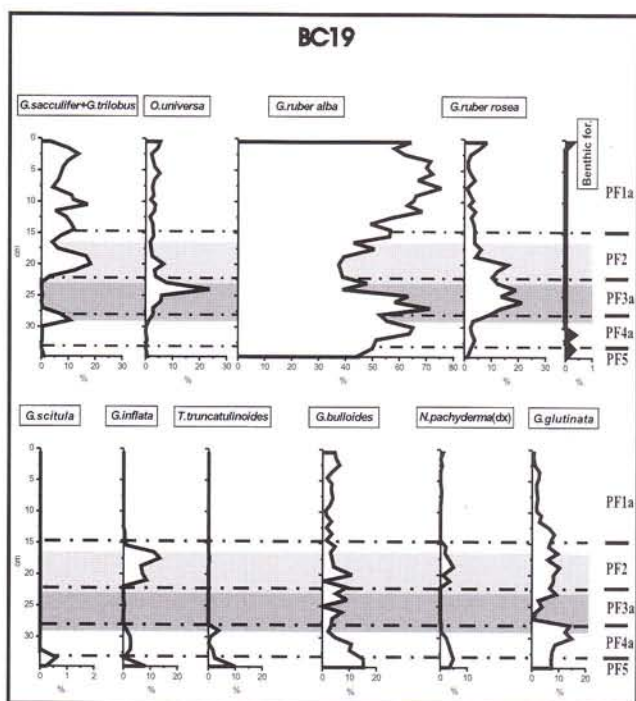


Fig. 3 - Relative frequencies (%) of selected planktonic foraminiferal species and total benthic foraminifera abundance (%) in BC19 box core. The defined assemblage zones are indicated in the right side. Horizontal scale of benthic forams abundance curve is expanded because of very low percentages.

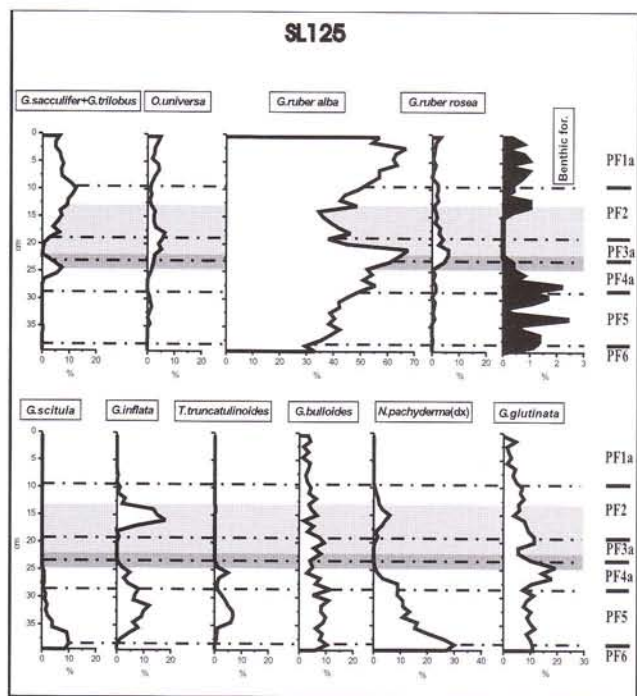


Fig. 4 - Relative frequencies (%) of selected planktonic foraminiferal species and total benthic foraminifera abundance (%) in SL125 box core. The defined assemblage zones are indicated in the right side. Horizontal scale of benthic foraminifera abundance curve is expanded because of very low percentages.

Sand fraction is usually high in correspondence of these cineritic levels (>50% in BC09 and >20% in BC19), whereas carbonate content is lower (~27.3% in BC09 and <20% in BC19). The colour of tephra layers is usually brownish-black.

### High-resolution biostratigraphic scheme for the eastern Mediterranean: planktonic foraminiferal assemblage zones

The scheme proposed in this paper is based on major compositional changes in planktonic foraminiferal assemblages from the Ionian Sea and the Levantine Basin. It consists of 6 assemblage zones, indicated by "PF" ("Planktonic Foraminifera") and progressive numbers, starting from the most recent interval recognised. The "a" and "b" codes which sometimes follow the number of the assemblage zone are used to distinguish regional differences in planktonic association and they define assemblage subzones. The relative frequency patterns of the dominating species in the various cores are shown in Figs. 3 to 9.

PF assemblages in all the studied cores are comparable: the changes (abundance variation, presence/absence) which characterise the assemblage zones are the same in each zone. In fact, although the relative abundances of the various species differ between the cores, increases, decreases and abundance peaks of marker species always occur in the same stratigraphic position and are probably synchronous.

The assemblage zones are defined as follows, starting from the oldest interval recognised:

#### Assemblage zone PF6

This interval is identified below sapropel S1. This assemblage zone was identified as follows: from 38 cm to the bottom of the core in box-core SL125 (Fig. 4), from 39 cm to the bottom of the core in BC06 (Fig. 6) and from 38 cm to the bottom of the core in BC09 (Fig. 9).

Base of interval: not defined.

Significant trends: planktonic foraminiferal association is characterised by the dominance of cold-water species (Bé & Tolderlund 1971; Thunell 1978) such as right-coiled *N. pachyderma* and *G. scitula*. The assemblage also consists of other species living in colder water such as *T. quinqueloba* (not reported in Figs. 3-9), *G. bulloides* and *G. glutinata*, an opportunistic species widespread in the Mediterranean Sea (Thunell 1978). At the same time there is a marked decrease in abundance of *G. ruber* (var. *alba*), the principal component of the tropical-subtropical association (Hemleben et al. 1989; Rohling et al. 1993) in this interval; it shows an increase in abundance only near the upper boundary of the interval.

#### Assemblage zone PF5

This interval was recognised in all the box cores (Figs. 3-9) as follows: from 33 cm to the bottom of the core in box-core BC19, from 28.5 cm to 38 cm in SL125, from 28 cm to the bottom of the core in BC07, from 29 cm to 39 cm in BC06, from 37 cm to the bottom of the core in BC02, from 29 cm to the bottom of the core in UM42 and from 32 cm to 38 cm in BC09.

Base of interval: appearance of *G. inflata* and *T. truncatulinoides*.

Significant trends: decreasing abundance of the subpolar species *G. scitula*. Presence of right coiled *N. pachyderma* with a clear increase of this species near the upper boundary of the interval. Significant percentage of *G. ruber* (var. *alba*) which shows a clear decrease in the upper part of the interval. Increase in abundance of *G. inflata* and *T. truncatulinoides*. In particular *T. truncatulinoides* seems to reproduce near the surface in winter and can sink to great depths during the growth (>1000 m, Hemleben et al. 1989). A deep vertical mixing is required to return individuals to surface waters. Abundance peaks of *G. inflata* are usually related to seasons of strong vertical mixing and a consequently homothermal water-column (Tolderlund & Bé 1971; Pujol & Vergnaud-Grazzini 1989).

#### Assemblage zone PF4

This interval is present in all the box cores (Figs. 3-9) as follows: from 27.8 cm to 33 cm in box-core BC19, from 22.8 to 28.5 cm in SL125, from 25.5 cm to 28 cm in BC07, from 25 cm to 29 cm in BC06, from 33 cm to 37 cm in BC02, from 27.5 cm to 29 cm in UM42 and from 26 to 32 cm in BC09.

Base of interval: *G. ruber* (var. *alba*) increase with values >50% (Levantine Basin cores) (PF4a)  $\geq$ 40% (Ionian sea cores) (PF4b). Contemporary appearance (PF4a) or presence (PF4b) of *G. ruber* (var. *rosea*).

Significant trends: presence of *G. inflata*, *T. truncatulinoides* and right coiled *N. pachyderma*. Increase in abundance of *G. sacculifer* in the upper part of the interval. As reported in Fenton et al. (2000), *G. sacculifer* thrives only in areas where the pycnocline is shallow, near the base of the photic zone, for instance because of strong runoff. In particular the preferred level of reproduction of this species usually coincides with the Deep Chlorophyll Maximum (DCM).

#### Assemblage zone PF3

This interval was recognised in all the studied box cores (Figs. 3-9) as follows: from 22 cm to 27.8 cm in box-core BC19, from 18.5 cm to 22.8 cm in SL125, from 21 to 25.5 cm in BC07, from 18.5 to 25 cm in BC06, from 28 cm to 33 cm in BC02, from 24.5 to 27.5 cm in UM42 and from 22.5 to 26 cm in BC09.

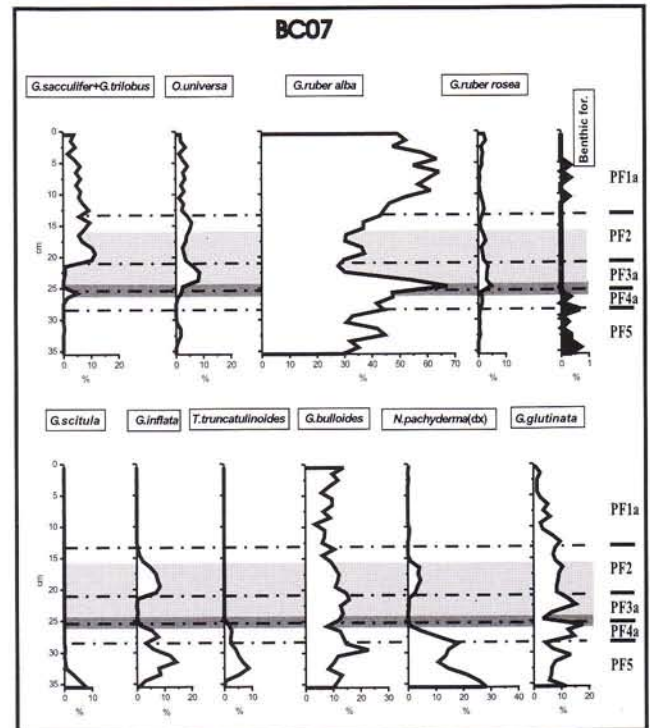


Fig. 5 - Relative frequencies (%) of selected planktonic foraminiferal species and total benthic foraminifera abundance (%) in BC07 box core. The defined assemblage zones are indicated in the right side. Horizontal scale of benthic foraminifera abundance curve is expanded because of very low percentages.

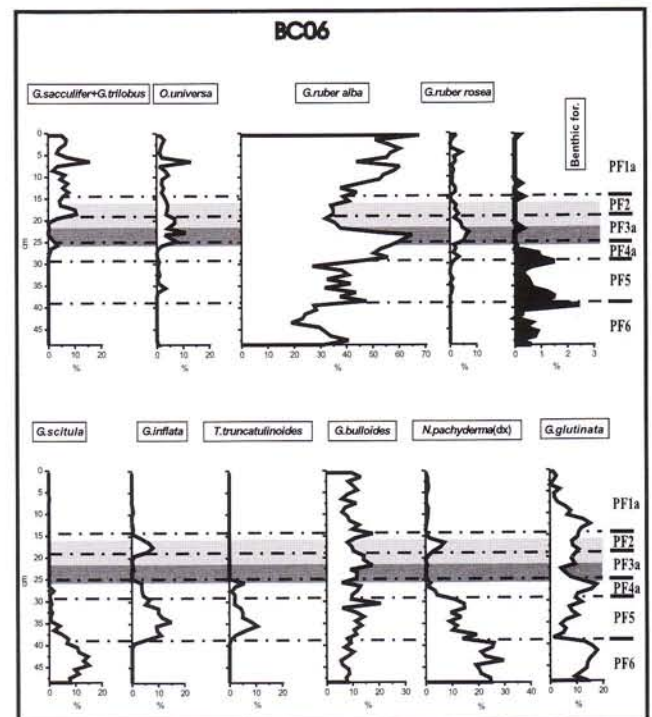


Fig. 6 - Relative frequencies (%) of selected planktonic foraminiferal species and total benthic foraminifera abundance (%) in BC06 box core. The defined assemblage zones are indicated in the right side. Horizontal scale of benthic foraminifera abundance curve is expanded because of very low percentages.

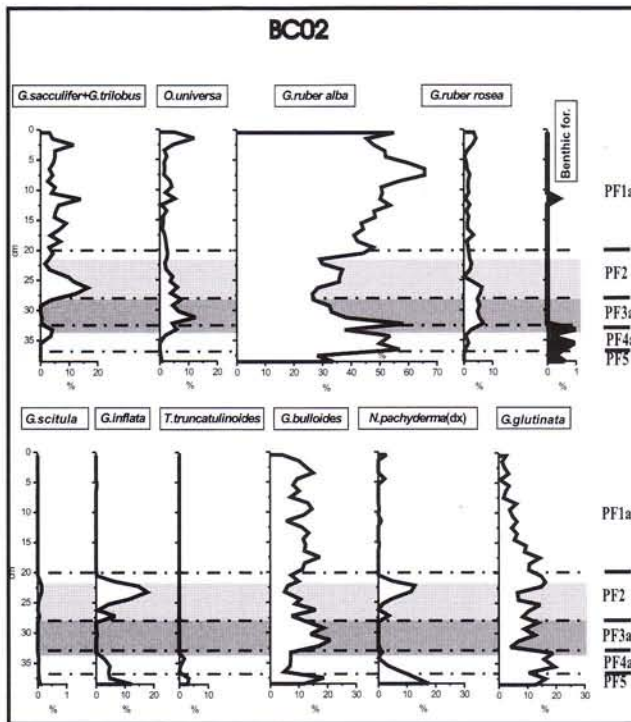


Fig. 7 - Relative frequencies (%) of selected planktonic foraminiferal species and total benthic foraminifera abundance (%) in BC02 box core. The defined assemblage zones are indicated in the right side. Horizontal scale of *G. scitula* and benthic foraminifera abundance curves are expanded because of very low percentages.

**Base of interval:** temporary disappearance of *G. sacculifer*, *G. inflata* and right coiled *N. pachyderma* (PF3a); significant decrease / temporary disappearance of *G. sacculifer*, *G. inflata* and right coiled *N. pachyderma* (PF3b). Disappearance of *T. truncatulinoides* (PF3a), temporary disappearance of *T. truncatulinoides* (PF3b). In both the PF3a and PF3b assemblage zones, temporary disappearance of all benthic foraminifera.

**Significant trends:** increase of *G. ruber* (var. *rosea*) and *O. universa*. Maximum abundance of *G. ruber* (var. *alba*). In particular the planktonic foraminiferal assemblage shows the disappearance of *G. sacculifer*. According to Fenton et al. (2000), in areas where adverse conditions (i.e. low oxygen) occur in the shallow mesopelagic zone, *G. sacculifer* seems to be at a competitive disadvantage compared to the shallow epipelagic species *G. ruber*. The problem of the *G. ruber* / *G. sacculifer* relationship is more complicated than a simple competition. It implies metabolic activity and different  $^{13}\text{C}$  incorporation as function of marine carbonate ion concentration and pH of sea water. For instance *G. ruber* seems to be almost two times more sensitive to changes in the carbonate chemistry than *G. sacculifer* even if both species live in the same habitat and have similar seasonal distributions (Bijma et al. 1998; Spero et al. 1998). The *rosea* variety of *G. ruber* shows a major increase in abundance in the eastern cores with respect

to the western cores; in fact in the easternmost core BC19, percentages values of this variety exceed 10%. Moreover it is possible to observe positive trend in abundance of the species *G. bulloides*. According to Ganssen & Kroon (2000), *G. bulloides* is a species typical of the spring bloom and it is considered a characteristic eutrophic species reaching its main occurrence in high-nutrient environments and during phytoplankton blooms, reflecting general conditions of enhanced productivity. Bijma et al. (1991) suggest that this species is able to survive in late upwelling systems, that is at the end of phyto- and zooplankton blooms, when oxygen has been rapidly consumed.

#### Assemblage zone PF2

This interval was recognised in all the studied cores (Figs. 3-9) as follows: from 14.5 to 22 cm in box-core BC19, from 9.5 to 18.5 cm in SL125, from 13 to 21 cm in BC07, from 14 to 18.5 cm in BC06, from 20 to 28 cm in BC02, from ca. 6 to 24.5 cm in UM42, which includes a supposed reworked level and a tephra layer at the upper boundary of interval, and from 10 to 22.5 cm in BC09.

**Base of interval:** clear increase in abundance of *G. sacculifer*, reappearance of *G. inflata* and right coiled *N. pachyderma*.

**Significant trends:** presence of warm water species such as *G. sacculifer* and *O. universa*, usually included by cluster analysis in the same group (SPRUDTS group; Rohling et al. 1993), and *G. ruber* (var. *alba* and *rosea*). The upper part of the interval is characterised by the reappearance and following increase in abundance of *G. inflata* and right coiled *N. pachyderma*.

#### Assemblage zone PF1

This interval was recognised in all the studied cores (Figs. 3-9) as follows: from the top to 14.5 cm in box-core BC19 with a tephra layer in the lower part of interval, from the top to 9.5 cm in SL125, from the top to 13 cm in BC07, from the top to 14 cm in BC06, from the top to 20 cm in BC02, from the top to ca. 6 cm in UM42 and from the top to 10 cm in BC09, with a tephra layer in the lower part of interval.

**Base of PF1a interval:** disappearance of *G. inflata* and right coiled *N. pachyderma* (PF1a) (Figs. 3-7).

**Base of PF1b interval:** significant decrease (UM42; Fig. 8) or temporary disappearance (BC09; Fig. 9) of right coiled *N. pachyderma* and temporary disappearance of *G. inflata*. In UM42 this boundary is not defined with confidence because of re-sedimentation above S1.

**Significant trends:** presence of warm-water species such as *G. sacculifer*, *O. universa* and *G. ruber* (var. *alba*). *G. ruber* (var. *rosea*) is also present in this interval, but with abundance values clearly lower than in the sapropel; this is visible in cores from the Levantine Basin (PF1a).

*G. bulloides* and *G. glutinata* are also present in the foraminiferal assemblage in both the PF1a and PF1b assemblage zones. The generally sporadic presence of *G. inflata* and *T. truncatulinoides* until the top of the interval, distinguishes the assemblage zone PF1b from the correspondent assemblage zone PF1a.

#### Comparison with previous studies related to the central Mediterranean

Figure 10 shows the comparison between assemblage zones (left side) identified in this paper for the eastern Mediterranean and the already existing biozonation (right side) defined for the central Mediterranean by Jorissen et al. (1993), Capotondi et al. (1999) and Sbaffi et al. (2001). In particular Jorissen et al. (1993) proposed a subdivision of the late Quaternary into three intervals defined by planktonic and benthonic foraminiferal distribution in deep-sea cores mostly recovered in the south-central Adriatic. Three different climatic stages are identified by major faunal changes: a glacial phase (Zone III), a transitional phase (Zone II) and a postglacial phase (Zone I). Radiocarbon chronology of the three Adriatic cores reported by Jorissen et al. (1993) shows an age of 12,700 yrs BP for the III/II boundary and of 9600 yrs BP for the II/I boundary. A detailed biozonation of the Late Quaternary is reported in the Capotondi et al. (1999) paper; these authors based their study on ca. 60 cores collected from the Adriatic and Tyrrhenian Seas. A succession of 10 "ecozones" characterised by different planktonic foraminiferal assemblages were defined for the last 23,000 yrs BP (radiocarbon age). All the ecozones recognised by Capotondi et al. were also detected in this study, although some different regional characteristics can be identified. Minor differences in the biozonation of the central and eastern Mediterranean are certainly due to the different size fraction used in the Capotondi et al. (1999) paper ( $>63 \mu\text{m}$ ) and in this study ( $>150 \mu\text{m}$ ). A revised biozonation, based on the study of two different planktonic groups (foraminifera and calcareous nannofossils) and on pteropod relative abundances and fluxes from Tyrrhenian cores, was proposed by Sbaffi et al. (2001). These authors adopt a revised biozonation for the central Mediterranean, following and integrating previous biostratigraphic schemes already suggested for this area by various authors (Jorissen et al. 1993; Tamburini et al. 1998; Asioli et al. 1999; Capotondi et al. 1999). In Fig. 10 only two radiocarbon ages of the Sbaffi et al. (2001) biostratigraphic scheme are reported: 14,700 yrs BP (5/6a boundary) and 6100 yrs BP (1b/2 boundary). The intervals 2, 3, 4 and 5 of Sbaffi et al. (2001) were not distinguished in Fig. 10 because it is not possible to find an exact correspondence between each biozone and the assemblage zones of this study on the basis of the planktonic foraminiferal species. Discrepan-

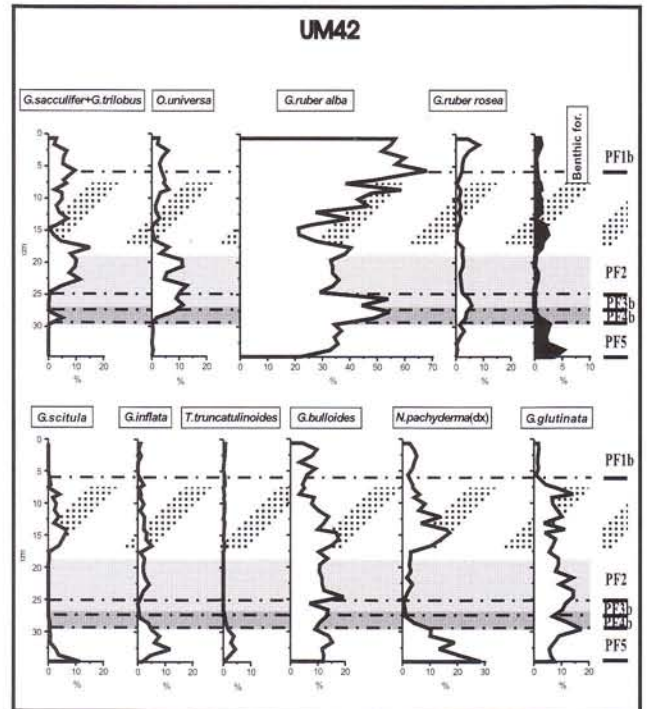


Fig. 8 - Relative frequencies (%) of selected planktonic foraminiferal species and total benthic foraminifera abundance (%) in UM42 box core. The defined assemblage zones are indicated in the right side. Horizontal scale of benthic foraminifera abundance curve is expanded because of very low percentages.

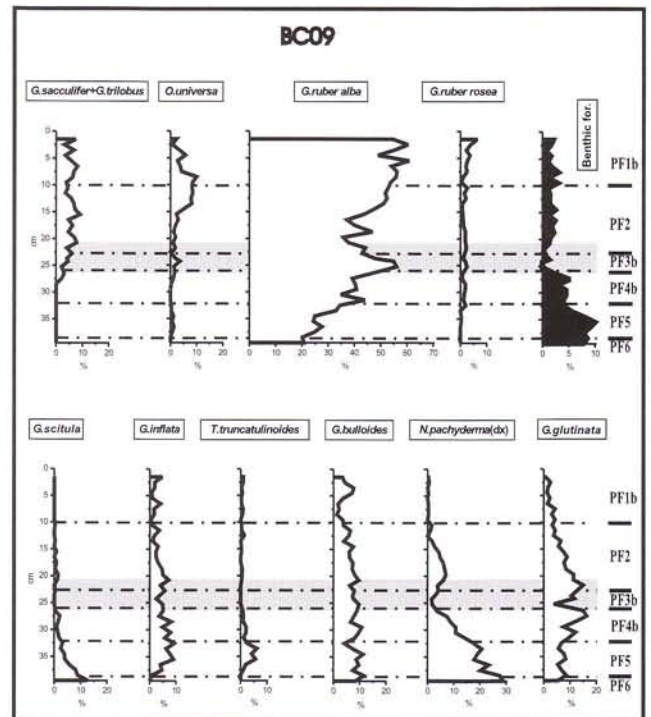


Fig. 9 - Relative frequencies (%) of selected planktonic foraminiferal species and total benthic foraminifera abundance (%) in BC09 box core. The defined assemblage zones are indicated in the right side. Horizontal scale of benthic foraminifera abundance curve is expanded because of very low percentages.

#### Assemblage zone PF5

This interval was recognised in all the box cores (Figs. 3-9) as follows: from 33 cm to the bottom of the core in box-core BC19, from 28.5 cm to 38 cm in SL125, from 28 cm to the bottom of the core in BC07, from 29 cm to 39 cm in BC06, from 37 cm to the bottom of the core in BC02, from 29 cm to the bottom of the core in UM42 and from 32 cm to 38 cm in BC09.

Base of interval: appearance of *G. inflata* and *T. truncatulinoides*.

Significant trends: decreasing abundance of the subpolar species *G. scitula*. Presence of right coiled *N. pachyderma* with a clear increase of this species near the upper boundary of the interval. Significant percentage of *G. ruber* (var. *alba*) which shows a clear decrease in the upper part of the interval. Increase in abundance of *G. inflata* and *T. truncatulinoides*. In particular *T. truncatulinoides* seems to reproduce near the surface in winter and can sink to great depths during the growth (>1000 m, Hemleben et al. 1989). A deep vertical mixing is required to return individuals to surface waters. Abundance peaks of *G. inflata* are usually related to seasons of strong vertical mixing and a consequently homothermal water-column (Tolderlund & Bé 1971; Pujol & Vergnaud-Grazzini 1989).

#### Assemblage zone PF4

This interval is present in all the box cores (Figs. 3-9) as follows: from 27.8 cm to 33 cm in box-core BC19, from 22.8 to 28.5 cm in SL125, from 25.5 cm to 28 cm in BC07, from 25 cm to 29 cm in BC06, from 33 cm to 37 cm in BC02, from 27.5 cm to 29 cm in UM42 and from 26 to 32 cm in BC09.

Base of interval: *G. ruber* (var. *alba*) increase with values >50% (Levantine Basin cores) (PF4a)  $\geq$ 40% (Ionian sea cores) (PF4b). Contemporary appearance (PF4a) or presence (PF4b) of *G. ruber* (var. *rosea*).

Significant trends: presence of *G. inflata*, *T. truncatulinoides* and right coiled *N. pachyderma*. Increase in abundance of *G. sacculifer* in the upper part of the interval. As reported in Fenton et al. (2000), *G. sacculifer* thrives only in areas where the pycnocline is shallow, near the base of the photic zone, for instance because of strong runoff. In particular the preferred level of reproduction of this species usually coincides with the Deep Chlorophyll Maximum (DCM).

#### Assemblage zone PF3

This interval was recognised in all the studied box cores (Figs. 3-9) as follows: from 22 cm to 27.8 cm in box-core BC19, from 18.5 cm to 22.8 cm in SL125, from 21 to 25.5 cm in BC07, from 18.5 to 25 cm in BC06, from 28 cm to 33 cm in BC02, from 24.5 to 27.5 cm in UM42 and from 22.5 to 26 cm in BC09.

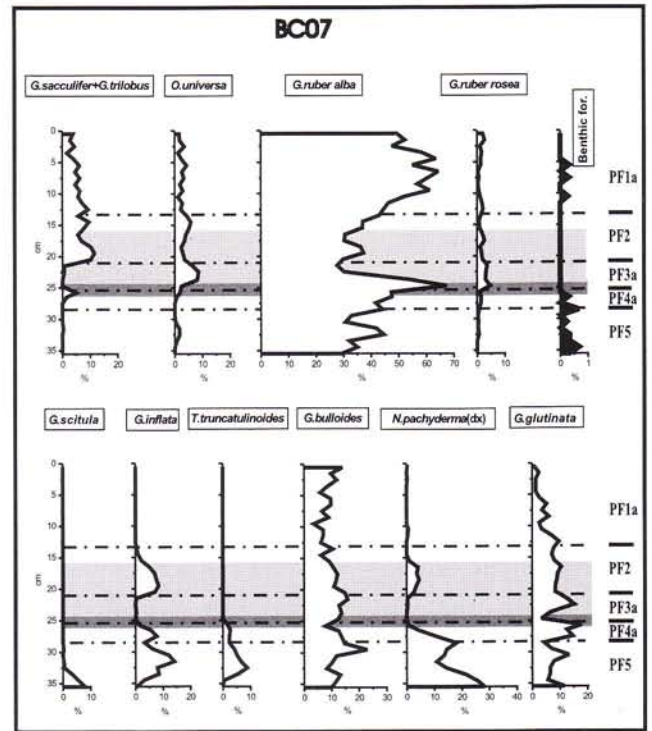


Fig. 5 - Relative frequencies (%) of selected planktonic foraminiferal species and total benthic foraminifera abundance (%) in BC07 box core. The defined assemblage zones are indicated in the right side. Horizontal scale of benthic foraminifera abundance curve is expanded because of very low percentages.

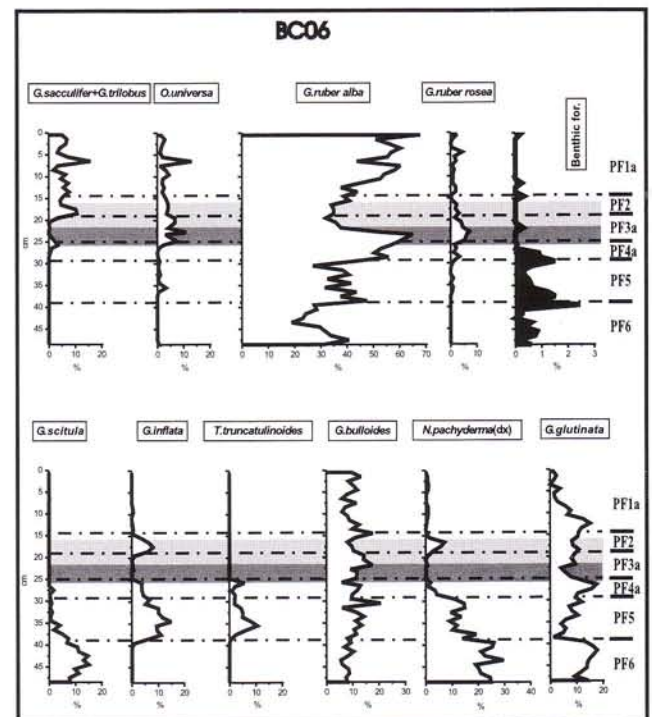


Fig. 6 - Relative frequencies (%) of selected planktonic foraminiferal species and total benthic foraminifera abundance (%) in BC06 box core. The defined assemblage zones are indicated in the right side. Horizontal scale of benthic foraminifera abundance curve is expanded because of very low percentages.

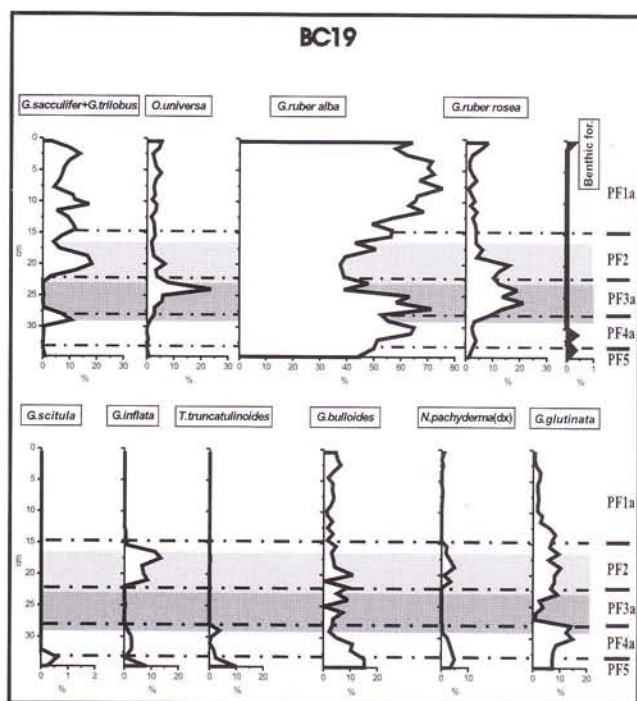


Fig. 3 - Relative frequencies (%) of selected planktonic foraminiferal species and total benthic foraminifera abundance (%) in BC19 box core. The defined assemblage zones are indicated in the right side. Horizontal scale of benthic forams abundance curve is expanded because of very low percentages.

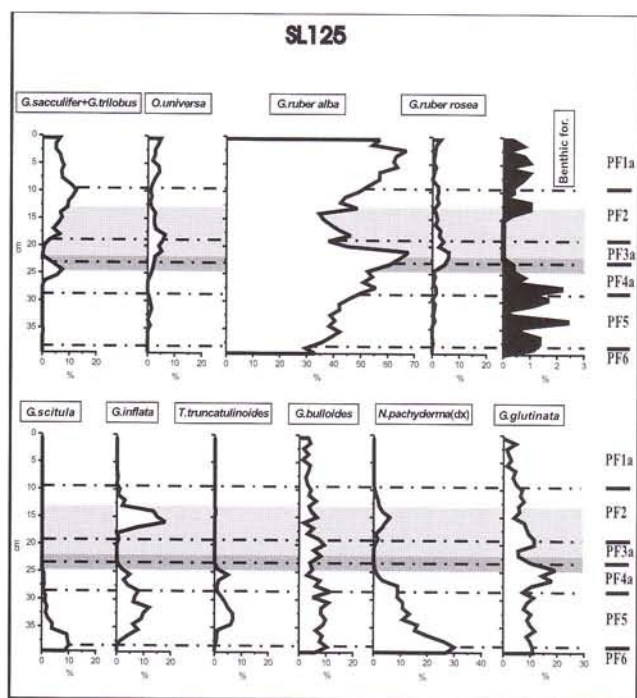


Fig. 4 - Relative frequencies (%) of selected planktonic foraminiferal species and total benthic foraminifera abundance (%) in SL125 box core. The defined assemblage zones are indicated in the right side. Horizontal scale of benthic foraminifera abundance curve is expanded because of very low percentages.

Sand fraction is usually high in correspondence of these cineritic levels (>50% in BC09 and >20% in BC19), whereas carbonate content is lower (~27.3% in BC09 and <20% in BC19). The colour of tephra layers is usually brownish-black.

### High-resolution biostratigraphic scheme for the eastern Mediterranean: planktonic foraminiferal assemblage zones

The scheme proposed in this paper is based on major compositional changes in planktonic foraminiferal assemblages from the Ionian Sea and the Levantine Basin. It consists of 6 assemblage zones, indicated by "PF" ("Planktonic Foraminifera") and progressive numbers, starting from the most recent interval recognised. The "a" and "b" codes which sometimes follow the number of the assemblage zone are used to distinguish regional differences in planktonic association and they define assemblage subzones. The relative frequency patterns of the dominating species in the various cores are shown in Figs. 3 to 9.

PF assemblages in all the studied cores are comparable: the changes (abundance variation, presence/absence) which characterise the assemblage zones are the same in each zone. In fact, although the relative abundances of the various species differ between the cores, increases, decreases and abundance peaks of marker species always occur in the same stratigraphic position and are probably synchronous.

The assemblage zones are defined as follows, starting from the oldest interval recognised:

#### Assemblage zone PF6

This interval is identified below sapropel S1. This assemblage zone was identified as follows: from 38 cm to the bottom of the core in box-core SL125 (Fig. 4), from 39 cm to the bottom of the core in BC06 (Fig. 6) and from 38 cm to the bottom of the core in BC09 (Fig. 9).

Base of interval: not defined.

Significant trends: planktonic foraminiferal association is characterised by the dominance of cold-water species (Bé & Tolderlund 1971; Thunell 1978) such as right-coiled *N. pachyderma* and *G. scitula*. The assemblage also consists of other species living in colder water such as *T. quinqueloba* (not reported in Figs. 3-9), *G. bulloides* and *G. glutinata*, an opportunistic species widespread in the Mediterranean Sea (Thunell 1978). At the same time there is a marked decrease in abundance of *G. ruber* (var. *alba*), the principal component of the tropical-subtropical association (Hemleben et al. 1989; Rohling et al. 1993) in this interval; it shows an increase in abundance only near the upper boundary of the interval.

cies in the ages of zone / boundaries between the reported schemes could be due to different dating methods (tephrochronology or radiocarbon analyses), to the use of radiocarbon ages without corrections ( $^{14}\text{C}$  BP ages) as reported by Jorissen et al. (1993) and by Capotondi et al. (1999) or to the use of techniques for the calibration of radiocarbon ages (cal  $^{14}\text{C}$  BP ages) as reported by Sbaffi et al. (2001).

The comparison scheme represented in Fig. 10 is based on principal faunal changes characterising planktonic foraminiferal assemblages of the late Pleistocene/Holocene in the Mediterranean area.

The assemblage zone PF6 could be compared with the Zone III (glacial stage) of Jorissen et al. (1993), with the ecozone 7 (lower part) and the ecozone 8 of Capotondi et al. (1999) and with the two biozones 6a and 6b of Sbaffi et al. (2001), because of the common presence of cold-temperate water species (Bè & Tolderlund 1971; Thunell 1978) such as *G. scitula*, *N. pachyderma* and *T. quinqueloba*. Anyway *G. scitula* in association with right coiled *N. pachyderma*, *G. bulloides* and other species is interpreted as a warmer assemblage, typical of some interglacial stages in the North Hemisphere high latitude, such as in the Leg 152 sites (East Greenland Margin) (Spezzaferri 1998). This suggests that the cold/glacial intervals in the Mediterranean Sea probably correspond to interglacial stages in the polar regions in term of temperature. Another common character of this interval is the decrease of *G. ruber* (var. *alba*) in the eastern as in the central Mediterranean.

The base of assemblage zone PF5, defined by the appearance of *G. inflata* and *T. truncatulinoides*, corresponds to Zone III/II transition of Jorissen et al. (1993) and to the boundary between biozone 5 and 6a of Sbaffi et al. (2001). Capotondi et al. (1999) show a non-simultaneous appearance of the two species *G. inflata* and *T. truncatulinoides* within Ecozone 7 of the central Mediterranean. In cores from the eastern Mediterranean the shift is not always visible as it may represent a very short interval, such as in SL125.

The clear increase in abundance of *G. ruber* (var. *alba*), used to define the base of the PF4 (a, b) assemblage zone, is also visible at the top of Zone II of Jorissen et al. (1993) and in the lower part of ecozone 5 of Capotondi et al. (1999). Abundance values of *G. ruber*, which are higher in eastern Mediterranean than in central Mediterranean cores, testify the beginning of a general warming stage (transitional to postglacial, according to Jorissen et al. 1993).

The temporary disappearance of *T. truncatulinoides* is one of the major faunal changes characterising the transition from PF4 to PF3 assemblage zones in the eastern Mediterranean and boundaries between Zone I and II of Jorissen et al. (1993) and ecozone 5 and 4 of Capotondi et al. (1999) in the central Mediterranean. Another important bioevent at the base of the PF3 (a, b)

assemblage zone is the temporary disappearance (and/or decrease) of *G. inflata* and right coiled *N. pachyderma*. These changes are also detected in cores from the central Mediterranean, with some regional variations. According to Capotondi et al. (1999), *G. inflata* shows low abundance values in the Tyrrhenian Sea cores (as in the Ionian Sea), whereas it is absent in the Adriatic (as in the Levantine Basin cores of this study). Sbaffi et al. (2001) show a shift in the decrease of *G. inflata* and *N. pachyderma* in the Tyrrhenian Sea: the first species shows a clear decrease in abundance at the base of biozone 4, whereas the second species shows a decrease at the base of biozone 3.

The reappearance (and/or increase) of *G. inflata* and right coiled *N. pachyderma* is the common character of the PF3/PF2 (this paper) and 4/3 (Capotondi et al. 1999) transition. According to Sbaffi et al. (2001), this bioevent is also diachronous in the Tyrrhenian Sea: the increase of *G. inflata* is visible within biozone 3, whereas the significant increase of *N. pachyderma* occurs at the base of biozone 2.

The base of the PF1a assemblage zone, defined for the Levantine Basin, is characterised by a clear faunal change: the disappearance of *G. inflata* and right coiled *N. pachyderma*. According to the foraminiferal content, it is possible to relate the assemblage zone PF1a, identified in the Levantine Basin (this paper), to ecozones 2 and 1, defined by Capotondi et al. (1999) for the southern Adriatic Sea (cores IN 68-5, AD91-17 and AD91-16). A correspondence between assemblage zone PF1b, identified in the Ionian Sea (this paper), and the ecozones 2 and 1 recognised by Capotondi et al. (1999) in the Tyrrhenian Sea (cores ET91-18, GT85-5 and PB91-2) can be observed, based on the presence of *G. inflata* and *T. truncatulinoides* in the most recent foraminiferal assemblage. The same correspondence was detected with biozones 1a-1b, defined for the Tyrrhenian Sea by Sbaffi et al. (2001).

### Paleoclimatic implications

Comparison of the marine records with the continental records (ice cores, palynological and dendrochronological datas, varves, historical news ecc.) may add significant information on the palaeoclimatic changes occurring in the late Pleistocene/Holocene. In particular PF zones identified in box-core BC19 (Levantine Basin) are here compared with a chronostratigraphic scheme reported in Orombelli & Ravazzi (1996) for the late Pleistocene / Holocene, obtained by  $^{14}\text{C}$  ages BP and based on continental records.

The following chronological boundaries from Orombelli & Ravazzi (1996) were used:

1. Oldest Dryas / Bolling: 13 kyrs BP

2. Bolling / Older Dryas: 12 kyrs BP
3. Older Dryas / Allerod: 11.8 kyrs BP
4. Allerod / Younger Dryas: 11 kyrs BP
5. Younger Dryas / Preboreal: 10 kyrs BP
6. Preboreal / Boreal: 9 kyrs BP
7. Boreal / Atlantic: 8 kyrs BP
8. Atlantic / Subboreal: 5 kyrs BP
9. Subboreal / Subatlantic: 2.5 kyrs BP

In the left side of the Fig.10 the chronological boundaries of the assemblage zones were reported for the box core BC19, using an average sedimentation rate of 2.8 cm/1000 years, calculated by dating the identified tephra Z2 ( $3356 \pm 18$  yrs BP; De Rijk et al. 1999). In particular the tephra deposition was considered as an instantaneous event and for this reason the thickness of tephra was not evaluated in sedimentation rate calculation.

Starting from the oldest interval, it is possible to observe the following succession of climatic episodes in the box core BC19 (Fig. 10):

Assemblage PF5 corresponds in the upper part of the assemblage zone to the beginning of the glacial phase of Younger Dryas, occurred at the end of Pleistocene.

Assemblage PF4a represents the Younger Dryas / Preboreal transition, characterised by a gradual increase of temperature; as indicated by an upward increasing trends of tropical-subtropical species such as *G. ruber* (var. *rosea*), *O. universa* and *G. sacculifer*, typical species of warming periods.

Assemblage PF3a corresponds to the Boreal-Atlantic, two periods characterised by warm and wet climate. During this interval the S1 sapropel is deposited in the whole eastern Mediterranean.

Assemblage PF2 consists of a planktonic foraminiferal association in the remaining part of Atlantic, ending in the Subboreal, a cold and wet period, during which S1 deposition ended. According to the supposed ages reported in Fig. 10 for the BC19 box core, this interval lasted approximately from 6900 to 4300 yrs BP. During this period a cold Holocene event (5000-6100 yrs BP; O'Brien et al. 1995) is documented in the ice core Summit from Greenland (GISP2) in correspondence of an increase in concentrations of marine salt and continental dust.

Assemblage PF1a lasts from Subboreal to Subatlantic and represents recent climatic conditions. In this interval various short cold events were historically documented in continental environment (cooling period of the Iron Age, Little Ice Age, among others, Veggiani 1994; van Geel et al. 1998), but they are not clearly recorded in the box core BC19 because of low sedimentation rate and bioturbation.

Discrepancies between chronological boundaries

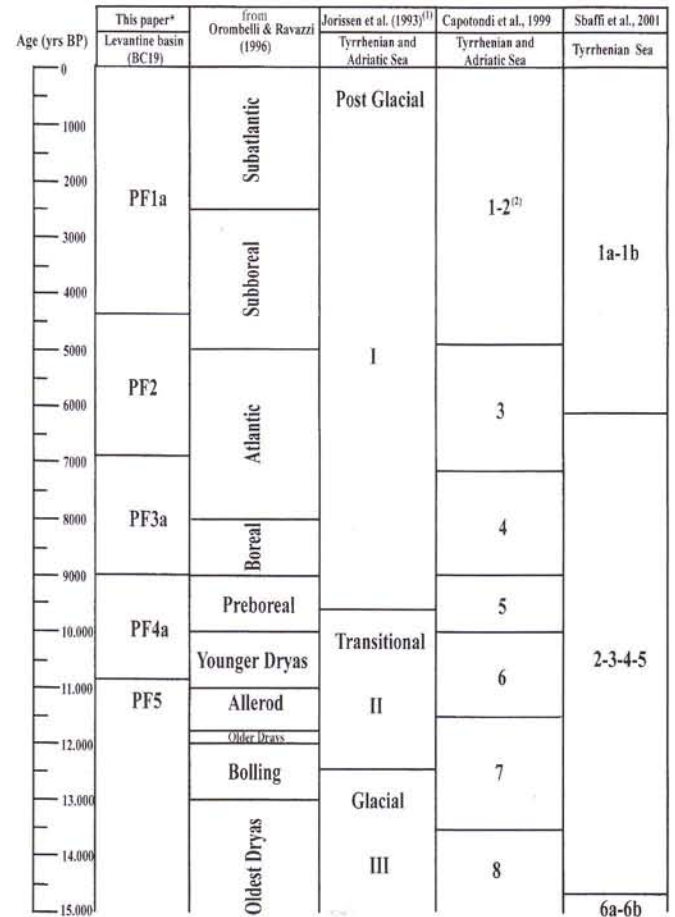


Fig. 10 - Comparison between planktonic foraminiferal assemblage zones from the box core BC19 in Eastern Mediterranean (this paper), a chronostratigraphic scheme from Orombelli & Ravazzi (1996) and the biozonation defined for Central Mediterranean (Jorissen et al. 1993; Capotondi et al. 1999; Saffi et al. 2001). The chronology of the assemblage zones boundaries defined in this paper for the Levantine Basin, on the left side, is based on tephrochronology. (\*) Supposed ages assuming an average sedimentation rate of 2.8 cm/ 1000 yrs for the box core BC19 on the base of Z2 tephra dating ( $3356 \pm 18$  yrs BP; De Rijk et al. 1999). The ages of the chronozones and the biozones defined for the central Mediterranean is based on radiocarbon analyses ( $^{14}\text{C}$  BP for Orombelli & Ravazzi 1996, Jorissen et al. 1993, Capotondi et al. 1999; cal  $^{14}\text{C}$  BP for Saffi et al. 2001). (1) Chronology of I/II and II/III boundaries based on IN 68-9 core (Adriatic sea; Jorissen et al. 1993). (2) Average age obtained by radiocarbon dating of the ecozone 2 base for Tyrrhenian sea (4000 yrs BP) and for Adriatic sea (5800 yrs BP) from Capotondi et al. (1999).

of planktonic foraminiferal assemblage zones and chronozones reported by Orombelli & Ravazzi (1996) can be explained by different response of continental and marine environments and/or by the assumption of constant sedimentation rates, based on one age control point only.

## Conclusions

The main results of the present study can be summarised as follows:

Qualitative and quantitative analyses of planktonic foraminiferal assemblages allow identification of successive bioevents, such as the temporary appearance/disappearance of species and their variation in abundance. Based on these bioevents six planktonic foraminiferal (PF) "assemblage zones" are identified. Differences are recognised between the Ionian Sea and the Levantine Basin in the most recent association.

Assemblage zones PF4, PF3 and PF2 represent planktonic foraminiferal associations just before, during and just after sapropel S1 deposition respectively, both in the Ionian Sea and in the Levantine Basin. In particular, the upper boundary of the PF2 assemblage zone always falls a few cm above the top of the oxidised layer of sapropel S1.

The S1 sapropel can be recognised in the eastern Mediterranean by planktonic foraminiferal assemblages even if no  $C_{org}$ -rich sediments are present (oxidised sapropel). In the box core BC09, located on the Medina Rise (Ionian Sea), the sudden disappearance of benthic foraminifera and the positive peak in abundance of the *G. ruber* group (var. *alba* and var. *rosea*), at the bottom of an oxidised layer, indicate that this level may be a completely oxidised S1.

The six assemblage zones identified in the eastern Mediterranean can be compared with the existing biostratigraphy of the central Mediterranean (Zones I-III of Jorissen et al. 1993; ecozones 1-8 of Capotondi et al. 1999 and biozones 1a-6b of Saffi et al. 2001). In summary, the successions of planktonic foraminifera in different areas of the Mediterranean Sea allow to conclude that the different biostratigraphical schemes developed in the central Mediterranean are also partially applicable in the eastern Mediterranean, with slight modifications. The interval corresponding to the sapropel S1 deposition as identified in this study (PF4-PF2 assemblage zones), is comparable with ecozones 6-3 of Capotondi et al. (1999). The most recent interval PF1 shows regional differences in planktonic association; in particular the recent foraminiferal assemblage of the Levantine Basin cores from this paper (PF1a) can be compared with the first two ecozones from Tyrrhenian Sea as defined by Capotondi et al. (1999), whereas the same interval in the Ionian cores (PF1b) can be also recognised in the Adriatic (Capotondi et al. 1999).

The comparison between the reported chronological scheme from Orbelli & Ravazzi (1996), based on continental records, and the assemblage zones defined for box core BC19 from the eastern Mediter-

anean, shows that the planktonic foraminiferal association (PF4a upper part) characterising the base of S1 may correspond to a climatic transition towards warmer conditions in continental environments (Preboreal period). The Climatic Optimum suggested by the PF3a assemblage in the eastern Mediterranean may correspond to a warm and wet stage in continental environments (Boreal-Atlantic period). The end of S1 deposition, characterised by the PF2 assemblage, includes the transition Atlantic-Subboreal in continental environments, when the climate changed from warm and wet to cold and wet.

*Acknowledgements.* I sincerely thank Comandante A. Lubrano and the entire crew of the R/V "Urania" for their assistance during the cruise SIN-SAP97, the chief scientist B. Della Vedova and all the scientific staff for their cooperation. I thank M.B. Cita and E. Erba for their critically reading of earlier versions of this manuscript; I also thank C. Corselli, I. Premoli Silva, A. Negri and W.J. Zachariasse for valuable discussions and suggestions and L. Vezzoli for tephra identification. I am grateful to G. J. De Lange for access to cores UM42, BC19 and SL125 and to E. Schefuss for washing samples of core UM42. Thanks to L.J. Lourens, S. Iaccarino and S. Spezzaferrì for their constructive review. Thanks are also due to Ben Walsworth-Bell for the English revision of the manuscript. Research Grant MURST "Climatic variability of past regimes"-SINAPSI and the European Project SAP (Contract MAS3-CT-97-0137) supported this manuscript.

## REFERENCES

- Asioli A., Trincardi F., Lowe J. & Oldfield F. (1999) - Short-term climate changes during the Last Glacial-Holocene transition: comparison between Mediterranean records and the GRIP event stratigraphy. *J. Quatern. Sci.*, 14, 4: 373-381, Harlow.
- Bé A.W.H. & Tolderlund D.S. (1971) - Distribution and ecology of living planktonic foraminifera in surface waters of the Atlantic and Indian Oceans. In: Funnel B.M. & Riedel W.R. (eds.) - *The Micropaleontology of oceans*, 105-149, Cambridge.
- Bijma J., Spero H.J. & Lea D.W. (1998) - Oceanic carbonate chemistry and foraminiferal isotopes: new laboratory results. 6<sup>th</sup> International Conference on Paleoceanography, *Abstract Vol.*, 78, Lisbon.
- Bijma J., Hemleben Ch., Oberhansly H. & Spindler M. (1991) - The effects of increased water fertility on tropical spinose planktonic foraminifera in laboratory cultures. In: Bijma J., Hans-Joachim Kohler, Druck & Reprografie, *On the biology of tropical Globigerinidae (Sarcodina, Foraminiferida) and its implications for paleoecology*, 99-141, Tübingen.
- Borsetti A.M., Capotondi L., Cati F., Negri A., Vergnaud-Grazzini C., Alberini C., Colantoni P. & Curzi P. (1995) - Biostratigraphic events and Late Quaternary tectonics in the Dosso Galignani (central-southern Adriatic Sea). *G. Geol.*, 57 (1-2): 41-58, Bologna.
- Calvert S.E. (1983) - Geochemistry of Pleistocene sapropels and associated sediments from the Eastern Mediterranean Sea. *Oceanol. Acta*, 6: 255-267, Montreuil.
- Capotondi L. (1995) - Biostratigraphic changes and paleoceanographic record in the Corsica Basin (Tyrrhenian Sea) during the last 18000 years. *Palaeopelagos*, 5: 215-226, Roma.
- Capotondi L., Borsetti A.M. & Morigi C. (1999) - Foraminiferal ecozones, a high resolution proxy for the late Quaternary biochronology in the central Mediterranean Sea. *Mar. Geol.*, 153: 253-274, Amsterdam.
- Capotondi L., Borsetti A.M., Vergnaud-Grazzini C. & D'Onofrio S. (1989) - Biostratigrafia e stratigrafia isotopica della carota AC 85-4: considerazioni sulla paleoceanografia tardo-quaternaria del Mar Tirreno orientale. *G. Geol.*, 51/1: 201-212, Bologna.
- Capotondi L. & Morigi C. (1996) - The last deglaciation in the South Adriatic Sea: biostratigraphy and paleoceanography, II. Quaternario. *Ital. J. Quat. Sci.*, 9(2): 679-686, Harlow.
- Cita M.B., Bossio A., Colombo A., Gnaccolini M., Salvatorini G., Camerlenghi A., Catrullo D., Clauzon G., Croce M., Giambastiani M., Kastens K.A., Malinverno A., McCoy F.W. & Parisi E. (1982) - Sedimentation in the Mediterranean Ridge Cleft (DSDP Site 126). *Mem. Soc. Geol. It.*, 24: 427-442, Roma.
- Cita M.B., Vergnaud-Grazzini C., Robert C., Chamley H., Ciaranfi N. & D'Onofrio S. (1977) - Paleoclimatic Record of a Long Deep Sea Core from the Eastern Mediterranean. *Quaternary Research*, 8: 205-235, New York.
- Coltelli M., Del Carlo P. & Vezzoli L. (1998) - Discovery of a Plinian eruption of Roman age at Etna volcano, Italy. *Geology*, 26: 1095-1098, Boulder.
- De Lange G.J., Middelburg J. J. & Pruyssers P.A. (1989) - Middle and Late Quaternary depositional sequences and cycles in the eastern Mediterranean. *Sedimentology*, 36: 151-158, Oxford.
- De Rijk S., Hayes A. & Rohling E.J. (1999) - Eastern Mediterranean sapropel S1 interruption: an expression of the onset of climatic deterioration around 7 ka BP. *Mar. Geol.*, 153: 337-343, Amsterdam.
- Dymond J. & Collier R. (1996) - Particulate barium fluxes and their relationships to biological productivity. *Deep-Sea Res.*, 11, 43: 1283-1308, Oxford.
- Emeis K.-C. & Shipboard Scientific Party (1996). Paleocyanography and sapropel introduction. *Proc. ODP, Init. Repts.*, 160: 21-28, College Station.
- Fenton M., Geiselhart S., Rohling E.J. & Hemleben C. (2000) - Aplanktonic zones in the Red Sea. *Mar. Micropaleontol.*, 40 (3): 277-294, Amsterdam.
- Freydier R., Michard A., De Lange G. J. & Thomson J. (2001) - Nd isotopic compositions of Eastern Mediterranean sediments: tracers of the Nile influence during sapropel S1 formation? *Mar. Geol. Sp. Iss.*, 177 (1,2): 45-62, Amsterdam.
- Ganssen G. M. & Kroon D. (2000) - The isotopic signature of planktonic foraminifera from NE Atlantic surface sediments implications for the reconstruction of past oceanic conditions. *Journ. of the Geol. Soc.* 157: 693-699, London.
- Hemleben Ch., Spindler M. & Anderson O.R. (1989) - Modern planktonic foraminifera. V. of 363 pp. Springer-Verlag Ed., New York.
- Hilgen F.J. (1991a) - Astronomical calibration of Gauss to Matuyama sapropels in the Mediterranean and implication for the geomagnetic polarity timescale. *Earth Planet. Sci. Lett.*, 104: 226-244, Amsterdam.
- Hilgen F.J. (1991b) - Extension of the astronomically calibrated (polarity) timescale to the Miocene/Pliocene boundary. *Earth Planet. Sci. Lett.*, 107: 349-368, Amsterdam.
- Hilgen F.J., Krijgsman W., Langereis C.G., Lourens L.J., Santarelli A. & Zachariasse W.J. (1993) - Evaluation of the astronomically calibrated time scale for the late Pliocene and earliest Pleistocene. *Paleoceanography*, 8: 549-565, Washington.
- Jorissen F.J., Asioli A., Borsetti A.M., Capotondi L., de Visser J.P., Hilgen F.J., Rohling E.J., van der Borg K., Vergnaud-Grazzini C. & Zachariasse W.J. (1993) - Late Quaternary central Mediterranean biochronology. *Mar. Micropaleontol.*, 21: 169-189, Amsterdam.
- Kidd R.B., Cita M.B. & Ryan W.B.F. (1978) - Stratigraphy of eastern Mediterranean sapropel sequences recovered during DSDP Leg 42A and their paleoenvironmental significance. In: Hsu K., Montadert L. et al.- *DSDP Init. Repts.*, 42A: 421-443, Washington.
- Lourens L.J., Antonarakou A., Hilgen F.J., Van Hoof A.A.M., Vergnaud-Grazzini C. & Zachariasse W.J. (1996) - Evaluation of the Plio-Pleistocene astronomical timescale. *Paleoceanography*, 11 (4): 391-413, Washington.
- O'Brien S.R., Mayewski P.A., Meeker L.D., Meese D.A.,

- Twickler M.S. & Whitlow S.I. (1995) - Complexity of Holocene climate as reconstructed from a Greenland ice core. *Science*, 270: 1962-1964, Washington.
- Orombelli C & Ravazzi C. (1996) - The Late Glacial and early Holocene: chronology and paleoclimate. *Il Quaternario*, 9 (2): 439-444, Roma.
- Pujol C. & Vergnaud-Grazzini C. (1989) - Paleooceanography of the Last Deglaciation in the Alboran Sea (Western Mediterranean). Stable isotope and planktonic foraminiferal records. *Mar. Micropaleontol.*, 15: 153-179, Amsterdam.
- Rohling E.J., Jorissen F.J., Vergnaud-Grazzini C. & Zachariasse W.J. (1993) - Northern Levantine and Adriatic Quaternary planktic foraminifera; Reconstruction of paleoenvironmental gradients. *Mar. Micropaleontol.*, 21: 191-218, Amsterdam.
- Rosignol-Strick M. (1985) - Mediterranean Quaternary-sapropels, an immediate response of the African monsoon to variation of insolation. *Palaeogeogr., Palaeoclimatol., Palaeoecol.*, 49: 237-263, Amsterdam.
- Sbaffi L., Wezel F.C., Kallel N., Paterne M., Cacho I., Ziveri P. & Shackleton N. (2001) - Response of the pelagic environment to palaeoclimatic changes in the central Mediterranean Sea during the Late Quaternary. *Mar. Geol.*, 178: 39-62, Amsterdam.
- Spero H.J., Lea D.W. & Bijma J. (1998) - Deconvoluting the planktonic foraminifera carbon isotope record. 6<sup>th</sup> International Conference on Paleoceanography, *Abstract Vol.*, 212, Lisbon.
- Spezzaferri S. (1998) - Planktonic foraminifer biostratigraphy and paleoenvironmental implications of Leg 152 sites (East Greenland Margin). *Proc. ODP, Scient. Res.*, 152: 161-189, College Station.
- Stanley D.J. & Maldonado A. (1977) - Nile Cone: Late Quaternary stratigraphy and sediment dispersal. *Nature*, 266: 129, London.
- Tamburini F., Sbaffi L., Wezel F.C. & McKenzie J.A. (1998) - Late Quaternary climatic variations on the Latium and Campanian Margin of the Tyrrhenian Sea. *Rend. Fis. Acc. Lincei*, 9, 9: 293-313, Roma.
- Thomson J., Higgs N.C., Wilson T.R.S., Croudace I.W., De Lange G.J. & Van Santvoort P.J.M. (1995) - Redistribution and geochemical behaviour of redox-sensitive elements around S1, the most recent eastern Mediterranean sapropel. *Geochim. Cosmochim. Acta*, 59: 3487-3501, Washington.
- Thomson J., Mercone D., De Lange J.G. & Van Santvoort P.J.M. (1999) - Review of recent advances in the interpretation of eastern Mediterranean sapropel S1 from geochemical evidence. *Mar. Geol.*, 153: 77-89, Amsterdam.
- Thunell R.C. (1978) - Distribution of recent planktonic foraminifera in surface sediments of the Mediterranean Sea. *Mar. Micropaleontol.*, 3: 147-173, Amsterdam.
- Tolderlund D.S. & Bé A.W.H. (1971) - Seasonal distribution of planktonic foraminifera in the western North Atlantic. *Micropaleontol.*, 17: 297-329, New York.
- Troelstra S.R., Ganssen G.M., Van der Borg K. & De Jong A.F.M. (1991) - A Late Quaternary stratigraphic framework for eastern Mediterranean sapropel S1 based on AMS 14C dates and stable oxygen isotopes. *Radiocarbon*, 33: 15-21, New Haven.
- Van Geel B., Raspopov O.M., van der Plicht J. & Renssen H. (1998) - Solar Forcing of Abrupt Climate Change around 850 calendar Years BC. In: "Natural catastrophes during Bronze Age civilisations". Peiser B.J., Palmer T. & Bailey M.E. (eds.). BAR International Series, 728: 162-168, Oxford.
- Van Santvoort P.J.M., De Lange G.J., Thomson J., Cussen H., Wilson T.R.S., Krom M.D. & Strohle K. (1996) - Active post-depositional oxidation of the most recent sapropel (S1) in sediments of the eastern Mediterranean Sea. *Geochim. Cosmochim. Acta*, 60: 4007-4024, Washington.
- Van Santvoort P.J.M. & De Lange G.J. (1997) - Geochemical and paleomagnetic evidence for the occurrence of "missing" sapropels in eastern Mediterranean sediments. *Paleoceanography*, 12, 6: 773-786, Washington.
- Veggiani A. (1994) - I deterioramenti climatici dell'età del ferro e dell'alto medioevo. In "Torricelliana", 45: 1-80, Faenza.
- Vergnaud-Grazzini C., Borsetti A.M., Cati F., Colantoni P., D'Onofrio S., Saliège J.F., Sartori R. & Tampieri R. (1988) - Paleooceanographic record of the last deglaciation in the Strait of Sicily. *Mar. Micropaleontol.*, 13: 1-21, Amsterdam.
- Vergnaud-Grazzini C., Capotondi L. & Lourens L.J. (1993) - A refined Pliocene to early Pleistocene chronostratigraphic frame at ODP Hole 653A (West Mediterranean). *Mar. Geol.*, 117: 329-349, Amsterdam.